Solution of the elliptic equation by a generalized multiscale finite element method in perforated media

{ Efendiev Yalchin, Spiridonov Denis, Maria Vasilyeva }   North-Eastern Federal University, Yakutsk, Russia

MULTISCALE MODEL REDUCTION AND HIGH PERFORMANCE COMPUTING LABORATORY

Introduction

In this work we consider the elliptic equation in perforated media for CG and mixed formulation. Nonhomogeneous boundary conditions on perforations can be considered for many applied problems. For example, the Robyn boundary conditions usually applied at the boundaries of the solid medium for reactive processes in porous media. For such processes we should resolve perforations and heterogeneity using very fine grid which leads to the large discrete systems and computationally expensive.
The classic method for solution of such problems on the coarse grid are a homogenization techniques[1]. The homogenization methods are used to construct the approximation of the problem on a coarse grid and allow to calculate the effective properties of the medium. In this method, an additional term is used for describing the pore-scale reaction on the coarse grid approximation. The multiscale methods can be applied for the coarse grid approximation by solution of the local problems and construction of the multiscale basis functions [2]. In this method we have a two-way information exchange between micro and macro levels. In this work, we use a generalized multiscale finite element method (GMsFEM) [3]. This method based on the calculation of the multiscale basis functions to reduce the dimension of the problem. For handling a boundary conditions on the perforations, in GMsFEM we construct the additional basis function, which improves the accuracy of the method.

CG GMFEM

In this section, we will describe construction local reduction of a model on the snapshot space by solving some local spectral problems with use GMsDGM.
First, we need to select subdomains ω_i and K_j, from our fine mesh. Then we solve partitions of unity in each K_j for all ω_i. The partitions of unity are linear functions. (fig. 2)

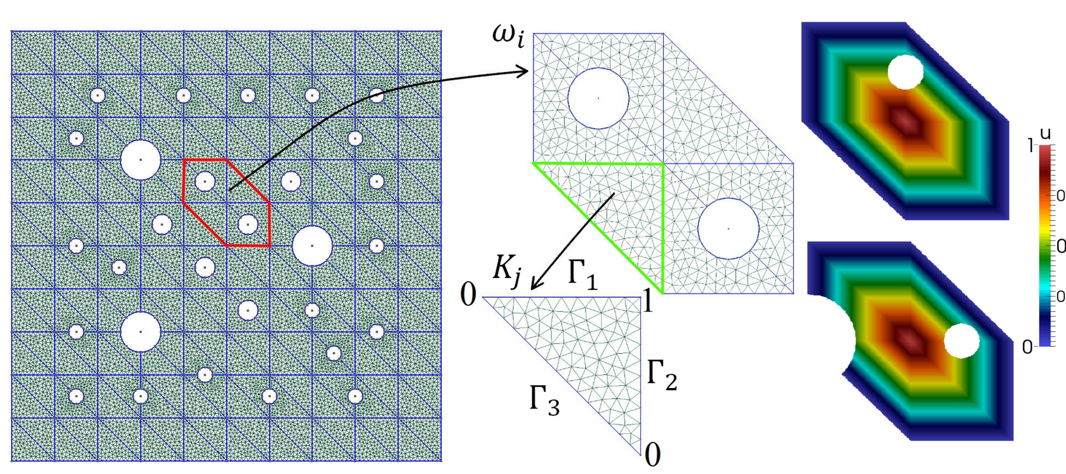

Figure 2: Subdomains ω_i, K_j and partitions of unity

Then we solve the following spectral problem in each ω_i:

$$A\varphi = \lambda S\varphi, \quad x \in \omega_i. \tag{6}$$

We must choose the first vectors φ, which correspond to L the first minimal eigenvalues λ. Variational formulations are defined below for matrices A and S, respectively.

$$a = \int_{\omega_i} (k\nabla u, \nabla q)dx, \quad s = \int_{\omega_i} (ku, q)dx$$

where q is test function.
This spectral problem we solve on the snapshot space which we obtain by solving the following problem:

For Dirichlet BC	For Robyn BC
$q\int_{\omega_i} k\nabla u\nabla v dx = 0,$	$\int_{\omega_i} k\nabla u\nabla v dx + \int_{\partial H} \alpha uv ds = 0$
$u = \delta_i, \quad x \in \partial\omega_i/\partial H,$	$u = \delta_i, \quad x \in \partial\omega_i/\partial H,$
$u = 0, \quad x \in \partial H.$	

Where δ_i is a function which in turn takes the value 1 at one point, and all other 0, ∂H - the boundary of perforations, $\partial\omega_i$ - the external boundary of ω_i.
After solving the spectral problem, we obtain the bases for the transition to the coarse grid space (fig. 3). In order to take into account boundary conditions on the perforations, we add the following additional basis in the ω_i regions where there are perforations(fig. 4):

For Dirichlet BC	For Robyn BC
$\int_{\omega_i} k\nabla u\nabla v dx = 0,$	$\int_{\omega_i} k\nabla u\nabla v dx + \int_{\partial H} \alpha uv ds = \int_{\partial H} \alpha f v ds$
$u = 0, \quad x \in \partial\omega_i/\partial H,,$	$u = 0, \quad x \in \partial\omega_i/\partial H,$
$u = 0, \quad x \in \partial\omega_i/\partial H.$	

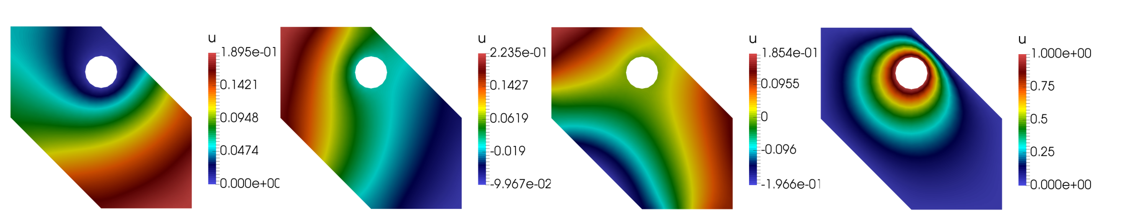

Figure 3: First three bases and additional basis for Dirichlet boundary conditions

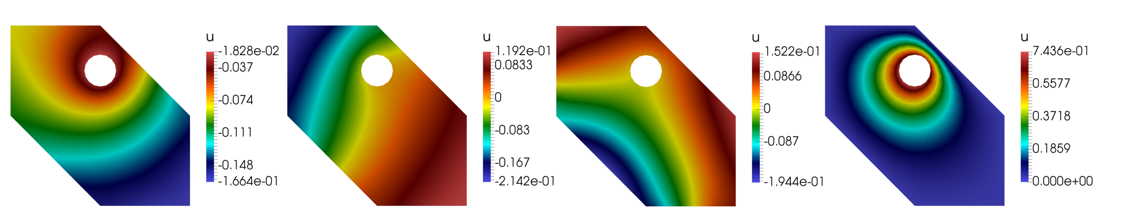

Figure 4: First three bases and additional basis for Robyn boundary conditions

CG GMsFEM Numerical results

We present a numerical results of problem with Dirichlet boundary conditions on perforations (1),(2) on fig. 5. The values of the coefficients are taken as follows: $k = 0.1$, $f = 1$. Relative errors in the L_2 and H_2 norm are presented in the table 1. As an exact solution, the FEM result was taken.

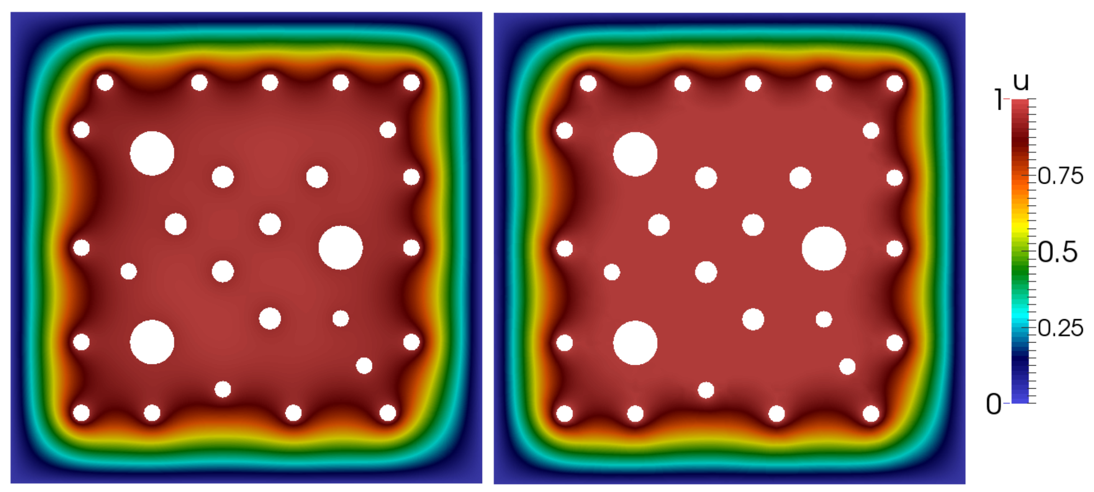

Figure 5: Numerical solutions with Dirichlet boundary conditions of FEM (left), GMsFEM (right)

Basis count	L_2 norm	H_1 norm
1	16.88	105.64
2	9.17	80.30
4	3.44	49.15
6	1.67	29.47
8	0.88	19.72
12	0.40	10.23
16	0.17	5.43

Table 1: The error of solution with Dirichlet boundary condition on perforations

The numerical results of problem with inhomogeneous Robyn boundary conditions on perforations (1),(3) on fig. 6. The values of the coefficients are taken as follows: $k = 0.1$, $f = 0$, $\alpha = 10$, $a = 1$. Relative errors in the L_2 and H_2 norm are presented in the table 2.

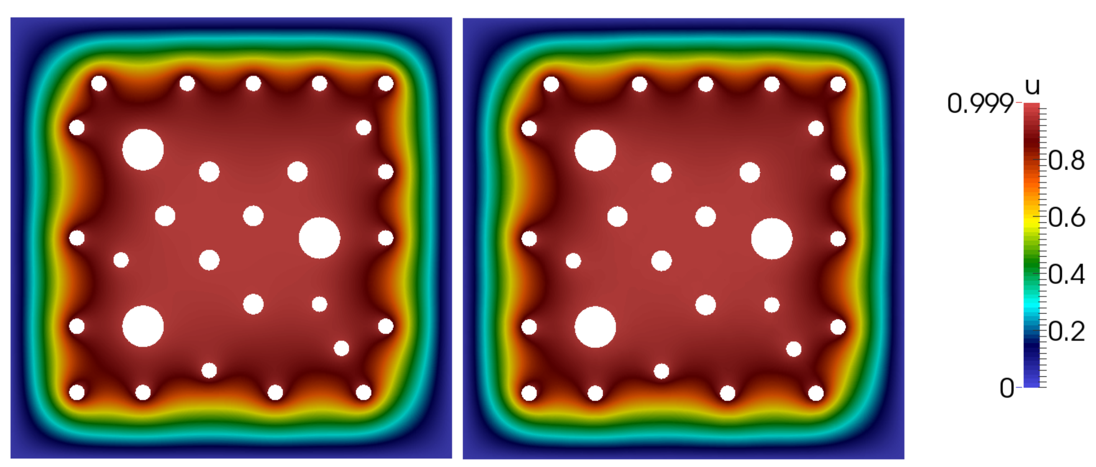

Figure 6: Numerical solutions with inhomogeneous Robyn boundary conditions of FEM (left), GMsFEM (right)

Basis count	L_2 norm	H_1 norm
1	10.25	73.21
2	4.04	46.59
4	1.77	27.87
6	0.78	14.37
8	0.50	10.75
12	0.21	5.65
16	0.11	3.64

Table 2: The error of solution with inhomogeneous Robyn boundary condition on perforations

Mathematical model

In this work we consider the standard elliptic equation

$$-\mathrm{div}(k\,\mathrm{grad}u) = f, \quad x \in \Omega. \tag{1}$$

We will solve this equation in two cases of boundary conditions. The first case is Dirichlet boundary condition on perforations:

$$\frac{\partial u}{\partial n} = 0, \quad x \in \Gamma_1, \qquad u = 1, \quad x \in \Gamma_p. \tag{2}$$

The second case is inhomogeneous Robyn boundary condition on perforeations:

$$\frac{\partial u}{\partial n} = 0, \quad x \in \Gamma_1, \qquad \frac{\partial u}{\partial n} = \alpha(u-a), \quad x \in \Gamma_P. \tag{3}$$

Our work also includes the solution of an elliptic equation in a mixed formulation

$$\begin{cases} k^{-1}q + \nabla c = 0 \\ \mathrm{div}q = 0 \end{cases}, \quad x \in \Omega, \tag{4}$$

with following boundary conditions:

$$q \cdot n = 0, \quad x \in \Gamma_1, \qquad c = g, \quad x \in \Gamma_P. \tag{5}$$

Where is Γ_P the boundary of perforations. Computational domain Ω is shown in fig.1

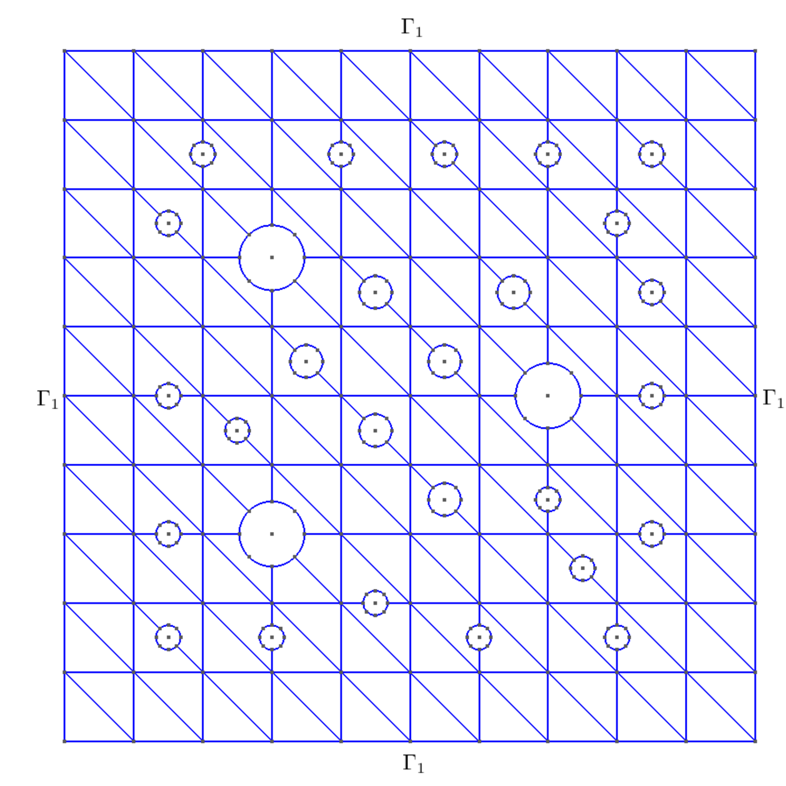

Figure 1: Computational domain

Mixed GMsFEM

In the case of mixed formulation, we have two unknowns flow q and concentration c functions. We compute basis function only for flow. Unlike the CG GMsFEM, the value of the flow is taken on the facets and therefore, in this case the ω_i region consists of subregions K_j around each coarse facet.
To compute basis we solve a spectral problem 6. But variational formulations for matrixes A and S will change:

$$a(u,v) = \int_{E_i} (u\cdot n)(v \cdot n)ds, \quad s(u,v) = \int_{\omega_i} uv dx + \int_{\omega_i} \mathrm{div}u\, \mathrm{div}v dx.$$

Where E_i is coarse facet on fine grid in ω_i. We solve the spectral problem on snapshot space which obtain from solving next local problem (fig. 7):

$$\begin{cases} k^{-1}q + \nabla c = 0 \\ \mathrm{div}q = 0 \end{cases}, \quad x \in \omega_i,$$

$$q \cdot n = 0, \quad x \in \partial\omega_i \cup \partial H$$
$$q \cdot n = \sigma_i, \quad x \in E_i$$

Where σ_i is a function which in turn takes the value 1 at one fine facet on, and all other 0. We need to compute smooth first basis separately, and additional basis to take into account boundary condition on perforations(fig 7):

$$\begin{cases} k^{-1}q + \nabla c = 0 \\ \mathrm{div}q = 0 \end{cases}, \quad x \in \omega_i,$$

For first basis	For additional basis
$q \cdot n = 1, \quad x \in E_i$	$q \cdot n = 1, \quad x \in \partial H$
$q \cdot n = 0, \quad x \in \omega_i$	$q \cdot n = 0, \quad x \in \omega_i$

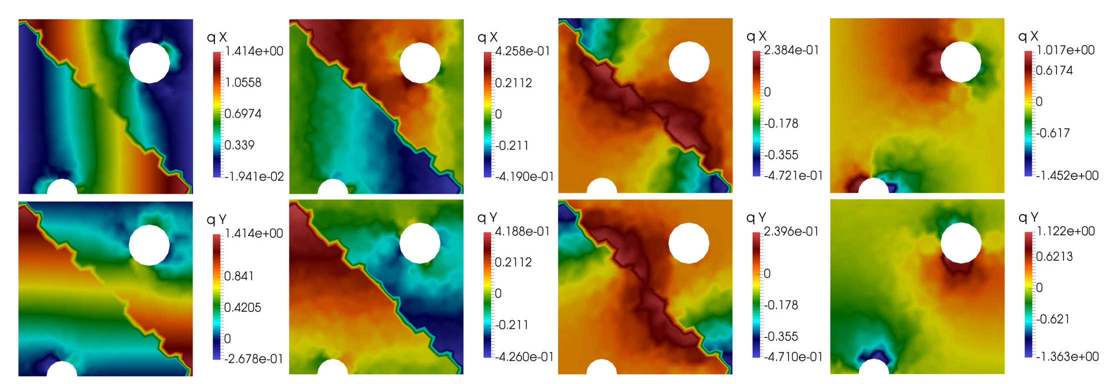

Figure 7: First three bases and additional basis

Mixed GMsFEM Results

We present a numerical results of mixed problem (4),(5) for flow and concentration on fig. 8 . The values of the coefficients are taken as follows: $k = 0.1, f = 1, g = 1$. Relative errors in the L_2 and H_2 norm are presented in the table 3 for flow, for concentration in the table 4. For concentration we compute error only in L_2 norm.

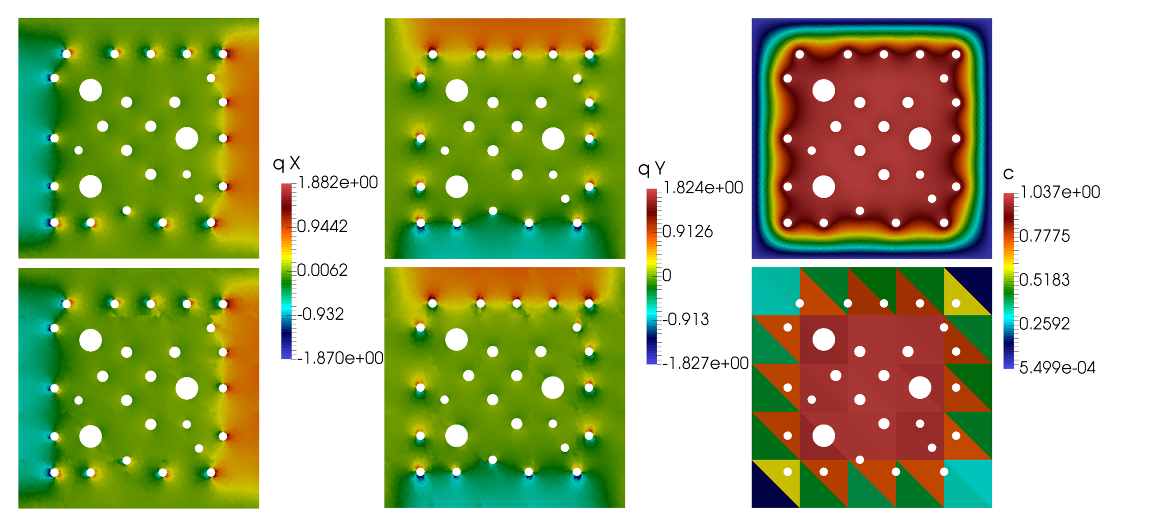

Figure 8: Numerical results of flow(1st and 2nd columns) and concentration (3rd column)(First row - FEM results, Second row - GMsFEM results

Basis count	L_2 norm	H_1 norm
1	134.11	90.73
2	6.27	4.24
3	0.90	0.61
4	0.54	0.36

Table 3: The error of result for flow

Basis count	L_2 norm
1	53.57
2	6.69
3	6.61
4	6.61

Table 4: The error of result for concentration

Conclusion and Future works

In this paper, we considered an elliptic equation in CG and mixed formulations. The results have good accuracy, the error decreases when number of bases increase. In the future we plan to use Robyn boundary conditions at the perforations for the mixed formulation and consider pore scale reactive flow.

References

[1] Bakhvalov N. S., Panasenko G. P. Homogenization of Processes in Nonhomogeneous media. – 1984.

[2] Efendiev Y., Hou T. Y. Multiscale finite element methods: theory and applications. – Springer Science & Business Media, 2009. – T. 4.

[3] Eric T. Chung, Yalchin Efendiev, Guanglian Li, Maria Vasilyeva. Generalized multiscale finite element methods for problems in perforated heterogeneous domains // Applicable Analysis. Volume 95, Issue 10, 2016. Pp. 2254-2279.

Contact Information

Web http://multiscalemr.ru
Email d.stalnov@mail.ru